A statistical framework for the robust detection of hidden variation in single cell transcriptomes

Donghyung Lee[1,*], Anthony Cheng[1,2], Mohan Bolisetty[1], and Duygu Ucar[1,3,*]

[1] The Jackson Laboratory for Genomic Medicine, Farmington, CT, USA.
[2] Department of Genetics and Genome Sciences, University of Connecticut Health Center, Farmington, CT, USA.
[3] Institute of Systems Genomics, University of Connecticut Health Center, Farmington, CT, USA.
* Correspondence: *donghyung.lee@jax.org* and *duygu.ucar@jax.org*

Abstract

Single cell RNA-sequencing (scRNA-seq) precisely characterize gene expression levels and dissect variation in expression associated with the state (technical or biological) and the type of the cell, which is averaged out in bulk measurements. Multiple and correlated sources contribute to gene expression variation in single cells, which makes their estimation difficult with the existing methods developed for bulk measurements (e.g., surrogate variable analysis (SVA)) that estimate orthogonal transformations of these sources. We developed iteratively adjusted surrogate variable analysis (IA-SVA) that can estimate hidden and correlated sources of variation by identifying a set of genes affected with each hidden factor in an iterative manner. Analysis of scRNA-seq data from human cells showed that IA-SVA could accurately capture hidden variation arising from technical (e.g., stacked doublet cells) or biological sources (e.g., cell type or cell-cycle stage). Furthermore, IA-SVA delivers a set of genes associated with the detected hidden source to be used in downstream data analyses. As a proof of concept, IA-SVA recapitulated known marker genes for islet cell subsets (e.g., alpha, beta), which improved the grouping of subsets into distinct clusters. Taken together, IA-SVA is an effective and novel method to dissect multiple and correlated sources of variation in scRNA-seq data.

Introduction

Single-cell RNA-Sequencing (scRNA-seq) enable precise characterization of gene expression levels, which harbour variation in expression associated with both technical (e.g., biases in capturing transcripts from single cells, PCR amplifications or cell contamination) and biological sources (e.g., differences in cell cycle stage or cell types). If these sources are not accurately identified and properly accounted for, they might confound the downstream analyses and hence the biological conclusions[1-3]. In bulk measurements, hidden sources of variation are typically unwanted (e.g., batch effects) and are computationally eliminated from

the data. However, in single cell RNA-seq data, variation/heterogeneity stemming from hidden biological sources can be the primary interest of the study; which necessitate their accurate detection (i.e., existence of a hidden factor) and estimation (i.e., contribution of this factor to the gene expression levels) for downstream data analyses and interpretation. For example, a recent such study uncovered a CD1C+ dendritic cell (DC) subset by profiling human blood samples[4] and improved the immune monitoring of human DCs in health and disease. One challenge in detecting hidden sources of variation in scRNA-seq data lies in the existence of multiple and highly correlated hidden sources, including geometric library size (i.e., the library size of log-transformed read counts), number of expressed genes in a cell, experimental batch effects, cell cycle stage and cell type[5-8]. The correlated nature of hidden sources limits the efficacy of existing algorithms to accurately detect the source and estimate its contribution to the variation in the data.

'Surrogate variable analysis' (SVA)[9-11] is a family of algorithms that are developed to detect and remove hidden and "unwanted" variation (e.g., batch effect) in gene expression data by accurately parsing the data into signal and noise. A number of SVA-based methods have been developed and used for the analyses of microarray, bulk, and single-cell RNA-seq data including SSVA[11] (supervised surrogate variable analysis), USVA[10] (unsupervised SVA), ISVA[12] (Independent SVA), RUV (removing unwanted variation)[13,14], and most recently scLVM[6] (single-cell latent variable model). These methods primarily aim to remove 'unwanted' variation (e.g., batch or cell-cycle effect) in data while preserving the biological signal of interest typically to improve downstream differential expression analyses between cases and controls. For this purpose, they utilize PCA (principal component analysis), SVD (singular vector decomposition) or ICA (independent component analysis) to infer orthogonal transformations of hidden factors that can be used as covariates in downstream analysis. However, this paradigm by definition results in orthogonality between multiple estimated factors and limits the efficacy of existing SVA-based methods for single-cell data analyses, in which some of the sources of variation are 'wanted' and are highly correlated with each other.

To fill this gap, we developed a robust and iterative SVA-based statistical framework: **I**teratively **A**djusted **S**urrogate **V**ariable **A**nalysis (IA-SVA) (Figure 1A and Methods for details), which provides three major advantages. First, it accurately estimates multiple hidden sources of variation even if the sources are correlated with each other and with known sources, which is a limitation of existing SVA-based methods. Second, it enables assessing the significance of each detected factor for explaining the unmodeled variation in the data. Third, it delivers a set of genes that are significantly associated with the detected hidden

source. Application of IA-SVA for scRNA-seq data analyses is diverse including the detection of "unwanted" variation due to cell contamination or "wanted" variation associated with rare cell types (Figure 1B). In simulation studies we showed that IA-SVA i) provides high statistical power in detecting hidden factors; ii) controls Type I error rate at the nominal level ($\alpha = 0.05$); iii) delivers high accuracy in estimating hidden factors. We evaluated the efficacy of IA-SVA on scRNA-seq data from human pancreatic islets and brain cells and showed that IA-SVA is effective in capturing heterogeneity associated with both technical (e.g., doublet cells) and biological sources (e.g., differences in cell types or cell-cycle stages). Furthermore, we showed that IA-SVA based gene selection can be further utilized in downstream analyses such as in data visualization using t-distributed stochastic neighbor embedding (tSNE) [15] and performs favourably compared to existing methods developed for gene selection and visualization (e.g., Spectral tSNE[16]).

Results

Benchmarking IA-SVA on simulated data.

To assess and compare the detection power, Type I error rate, and the accuracy of hidden source estimates using IA-SVA and existing state-of-the-art methods (i.e., USVA and SSVA), we performed simulation studies (see Methods for details) under the null hypothesis (i.e., a group (case/control) variable affecting 10% of genes and no hidden factor) and under the alternative hypothesis (i.e., a group variable and three hidden factors affecting 30%, 20%, 10% of genes, respectively). Under the alternative hypothesis, we considered two correlation scenarios where the three hidden factors are moderately ($|r|$=~0.3-0.6) or weakly ($|r|$<0.3) correlated with the group variable (i.e., a known factor). Under each simulation scenario, we generated 1,000 scRNA-seq data sets (10,000 genes and 50 cells) and performed IA-SVA, USVA and SSVA (α =0.05, 50 permutations) on them to detect simulated hidden factors. Using these simulation results, we assessed the empirical Type I error rate of each method (i.e., the number of times each method detects a false positive factor under the null hypothesis at the nominal level of 0.05 divided by the number of simulations (n=1,000)). Similarly, we also quantified the empirical detection power rate of each method under different alternative hypothesis scenarios as the number of times each method detects a simulated factor under the alternative hypothesis (i.e., a factor actually exists and is detected as significant by the method) divided by the number of simulations. We used the average of the absolute Pearson

correlation coefficients between the simulated and estimated hidden factors to quantify the accuracy of estimates.

Simulation studies showed that IA-SVA performs as well or better than USVA and SSVA in terms of detection power and accuracy of the estimate while controlling the Type I error rate (0.04 for IA-SVA versus 0.09 for USVA and SSVA) (Table 1). In particular, IA-SVA was more effective when a hidden factor affected a small percentage of genes and when the factors were correlated ($|r|$=0.3-0.6) with the known factor (i.e., group variable). For example IA-SVA detected Factor3, which affected only 10% genes, 87% of the time, whereas USVA and SSVA detected this factor 78% of the simulations (first three columns in Table 1). More importantly, IA-SVA correctly inferred the correlations among multiple hidden factors while USVA and SSVA delivered biased estimates due to their orthogonality assumption (Supplementary Figure S1).

IA-SVA captures variation stemming from a small number of alpha cells.

To test whether IA-SVA is effective in capturing variation within a homogenous cell population, we analysed scRNA-seq data generated from human alpha cells (n=101, marked with glucagon (*GCG*) expression) obtained from three diabetic patients[17] using the Fluidigm C1 platform[18], for which the original study did not report any separation of these alpha cells . Using geometric library size and patient ID as known factors, significant surrogate variables (SVs) were inferred using IA-SVA (α =0.05, 50 permutations) on the data (14,416 genes and 101 cells). For comparison, we applied PCA, USVA, and tSNE on this data. In USVA analysis, similarly geometric library size and patient ID were used as known factors and significant SVs were obtained (α =0.05, 50 permutations). In the PCA analysis, PC1 was discarded since it is highly correlated (r = 0.99) with the geometric library size.

Top two significant SVs inferred by IA-SVA clearly separated alpha cells into two groups (six outlier cells marked in red vs. the rest marked in grey at SV2 > 0.1) (Figure 2A). 27 genes significantly associated with second SV (SV2) (Benjamini-Hochberg q-value (FDR) < 0.05, coefficient of determination (R^2) > 0.6), which included genes expressed in fibroblasts such as *COL4A1* and *COL4A2*. These genes were exclusively expressed in six outlier cells and clearly separated alpha cells into two clusters (Figure 2B). A larger set of SV2-associated genes (n = 108, FDR < 0.05, R^2 > 0.3) was used for pathway and GO enrichment analyses and uncovered that these genes are associated with extracellular matrix receptors (Supplementary Table S1). Hence, these outlier cells likely arise from cell contamination (e.g., fibroblasts contaminating islet cells) or cell doublets (e.g., two cells captured together)

133 — a known problem in early Fluidigm C1 experiments[20,21]. Alternative methods (i.e., PCA,
134 USVA, tSNE) failed to clearly detect these outlier cells (Figure 2C-E).
135 We next studied whether this source of heterogeneity can be recapitulated in an
136 independent and bigger human islet scRNA-seq dataset[18], using gene expression profiles
137 (17,168 genes) of 569 alpha cells from six diabetic patients. Using geometric library size and
138 patient ID as known factors we identified top 2 significant SVs using IA-SVA and USVA.
139 For comparison, we also conducted PCA and tSNE analyses on this data. In PCA, PC1 was
140 discarded since it matched the geometric library size, which is adjusted for in IA-SVA and
141 USVA analyses. IA-SVA's SV2 separated alpha cells into two groups (Supplementary
142 Figure S2A) and as in the previous case it was associated with fibrotic response genes
143 including *SPARC, COL4A1, COL4A2* (n=81, FDR < 0.05 and R^2 > 0.3) (Supplementary
144 Figure S2B, GO/pathway results in Supplementary Table S2). These results highlight IA-
145 SVA's ability to detect variation among alpha cells potentially due to cell contamination or
146 cell doublets. PCA, USVA, and tSNE failed to clearly separate these compromised alpha
147 cells (Supplementary Figure S2C-E) from the rest of the cells.

148 **IA-SVA accurately detects variation arising from cell-cycle stage differences.**

149 Differences in cell-cycle stages lead to variation in single cell gene expression data[3].
150 Supervised methods based on SVA have been developed to detect and correct for cell cycle
151 stage differences, most notably the scLVM algorithm. scLVM implements a Bayesian latent
152 variable model to infer hidden cell-cycle factors by using known cell cycle genes[6]. IA-SVA
153 can provide an unsupervised alternative by accurately capturing cell-cycle related variation in
154 single cell data. To show this, we analyzed scRNA-seq data (21,907 genes and 74 cells)
155 obtained from human glioblastomas that has an established cell-cycle signature[22]. We
156 conducted IA-SVA analyses by using geometric library size as a known factor and extracted
157 top 2 significant SVs (α=0.05, 50 permutations). For comparison, we applied PCA, USVA
158 and tSNE analyses on this data, where for USVA geometric library size is used as a known
159 factor.
160 IA-SVA's SV1 clearly separated 13 cells from the rest (cells marked in red in Figure
161 3A), which was associated with 119 genes (FDR < 0.05 and R^2 > 0.3). Hierarchical clustering
162 (ward.D2, cutree_cols=2) using these genes confirmed the separation of cells into two groups
163 (Figure 3B), whereas alternative methods failed to clearly separate these two groups of cells
164 (Figure 3C-E). Pathway and GO enrichment analyses of these genes[23,24] revealed significant
165 enrichment for cell-cycle process related GO terms and pathways (Supplementary Table S3),

166 suggesting that this hidden variation is stemming from cell-cycle stage differences. Indeed,
167 cell-cycle-stage predictions of cells using the SCRAN R package[25] showed that cells in
168 different cell-cycle stages have different SV1 values (Figure 3F). We noted that SV1 is
169 highly correlated ($|r|$= 0.44) with the geometric library size (typically the top contributor to
170 the variation in single cell data), which might explain why alternative methods failed to
171 clearly detect this variation in the data. These results demonstrate that IA-SVA can
172 effectively detect variation stemming from cell-cycle differences in an unsupervised manner
173 from single cell transcriptomes, even if this factor is highly correlated with known factors.

174 **IA-SVA based gene selection improves single cell data visualization.**

175 tSNE and other dimension reduction algorithms (e.g., Spectral tSNE implemented in Seurat[16])
176 are frequently used to visualize single cell data since they group together cells with similar
177 gene expression patterns. However, variation introduced by technical or biological factors
178 can confound the signal of interest and generate spurious clustering of data. IA-SVA can be
179 particularly effective in handling this problem by estimating hidden factors of interest
180 accurately while adjusting for all known factors of no interest. Moreover, IA-SVA identifies
181 genes associated with each detected hidden factor, which could be biologically relevant such
182 as marker genes for different cell types. The genes inferred by IA-SVA can significantly
183 improve the performance of data visualization methods (e.g., tSNE[15]). To illustrate this, we
184 studied single cell gene expression profiles (16,005 genes) of alpha (n=101, marked with
185 glucagon (*GCG*) expression), beta (n=96, marked with insulin (*INS*) expression), and ductal
186 (n=16, marked with *KRT19* expression) cells obtained from three diabetic patients[17]. First, we
187 applied tSNE on all genes (n=16,005) and color-coded genes based on the reported cell type
188 assignments[17], which failed to separate cells from different origins (Figure 4A). Next, we
189 applied IA-SVA on this data using patient ID, batch ID and the number of expressed genes as
190 known factors and obtained significant SVs. SV1 and SV2 separated cells into distinct
191 clusters (Supplementary Figure S3), suggesting that these SVs might be associated with cell
192 type differences. Indeed, genes associated with SV1 and SV2 (n=92, FDR < 0.05 and R^2 >
193 0.5) included known marker genes used in the original study (*INS*, *GCG*, *KRT19*) and
194 uncovered alternative marker genes associated with alpha, beta and ductal cells (Figure 4B).
195 These genes were annotated with diabetes and insulin processing related GO terms and
196 pathways (Supplementary Table S4). As expected, tSNE analyses based on these 92 genes
197 improved data visualization and clearly grouped together cells with respect to their cell type
198 assignments (Figure 4C). Such improved analyses can be instrumental in discovering cells

199 that might be incorrectly labelled based on a single marker gene. For example, our analyses
200 revealed a beta cell that is labelled as a ductal cell in the original study (one green cell
201 clustered with blue cells in Figure 4C). For comparison, we applied recently developed
202 visualization methods, CellView[26] and Spectral tSNE[16], on the same data with their
203 recommended settings. CellView identified the 1000 most over-dispersed genes and
204 conducted tSNE on these genes. Spectral tSNE detected 2,933 most over-dispersed genes and
205 performed tSNE on significant principal components of these genes. On this small dataset,
206 both methods managed to group cells of different types into distinct groups (Supplementary
207 Figure S4), suggesting that existing methods for gene selection and visualization are effective
208 when datasets are small in size and are not confounded with multiple factors.

209 To test the efficacy of these methods on a bigger and more complex dataset, we
210 conducted similar analyses on scRNA-seq data (19,226 genes) of 1,600 islet cells including
211 alpha (n=946), beta (n=503), delta (n=58), and PP (n=93) cells from 6 diabetic and 12 non-
212 diabetic individuals, where the study includes multiple confounding factors (e.g., ethnicity,
213 disease state)[18]. We noted that original cell type assignments significantly correlate with
214 patient identifications (C=0.48, C=Pearson's contingency coefficient) and with ethnicity
215 (C=0.25), which would reduce the ability of existing methods to detect variation associated
216 with cell types. In such complex datasets, failing to properly adjust for potential confounding
217 factors prior to data analyses can lead to spurious grouping of cells, which might mislead the
218 biological conclusions. Indeed, when these cells were visualized using tSNE using all genes
219 (n=19,226) and were color-coded with respect to the original cell-type assignments [18], cell
220 types did not separate from each other and spurious clusters were observed within each cell
221 type (Figure 4D). As suspected, potential confounding factors (i.e., patient ID and ethnicity)
222 explained this grouping of cells (Supplementary Figure S5), which might be misleading as
223 researchers are looking for alpha and beta cell subtypes that can be related to Type 2 Diabetes
224 pathogenesis[27]. To eliminate spurious clusters stemming from known factors, existing
225 methods (e.g., Seurat) simply regress out all known factors prior to visualization. However,
226 this might affect the signal of interest (i.e., cell type assignment), due to high correlation
227 between known factors (i.e., patient ID) and the hidden factor (i.e., cell types).

228 We applied IA-SVA on this complex data, while accounting for known factors (i.e.,
229 the number of expressed genes and patient ID) and extracted top four significant SVs
230 (Supplementary Figure S6A and B). We identified 57 genes associated with the most
231 significant SV (SV1) (FDR < 0.05 and R^2 > 0.5), which included known marker genes (i.e.,
232 *INS* and *GCG*) (Supplementary Figure S7, Supplementary Table S5) and revealed novel

233 marker genes for these cell types. tSNE analyses using these 57 IA-SVA detected genes
234 clearly separated different cell types into discrete groups and reinforced the importance of
235 properly adjusting for known factors prior to data analyses (Figure 4E). For comparison, we
236 applied CellView and Spectral tSNE on this data with recommended settings; however they
237 failed to accurately group cells into distinct cell types (Figure 4F and G). Similar analyses
238 were conducted using PCA and USVA on the same data, where top surrogate factors
239 obtained with both methods failed to separate different cell types into distinct groups
240 (Supplementary Figure S6C and D). Combined together these analyses suggest that IA-SVA
241 is particularly effective in the analyses of complex datasets, which include the measurements
242 of many cells that are affected by diverse confounding factors.

243 Discussion

244 Surrogate variable analyses based methods are effective in detecting and eliminating hidden
245 and unwanted variation in bulk gene expression data (such as batch effects). By using
246 dimensionality reduction algorithms (e.g., PCA or SVD), these methods infer linear
247 transformations of hidden factors and utilize these factor estimates as additional covariates in
248 downstream analyses to eliminate unwanted variation[14]. However, measurement of gene
249 expression levels at single cell resolution pose novel challenges in the detection and
250 adjustment of hidden sources of data variation. First, single cell transcriptomes harbour
251 hidden variation that can be biologically interesting (hence 'wanted') and can be the major
252 goal of the study, for example detection of rare cells within a tissue[28] or detection of a cell's
253 subtypes that can be linked to health or disease[27]. Second, since single cell data do not
254 average out variation as in the case of bulk profiling, the data reflect variation arising from
255 diverse biological and technical sources some of which could be highly correlated. Existing
256 SVA-based methods do not readily apply to the unique needs of single cell data analyses. To
257 fill this gap, we developed IA-SVA, where the objective is the accurate estimation of hidden
258 factors even if these factors are correlated with each other or with the known factors. Unlike
259 other SVA-based methods, IA-SVA focuses more on the accurate detection and estimation of
260 hidden factors rather than their elimination since these factors can be biologically interesting,
261 e.g., identification of a new cell type and its marker genes. Indeed, analyses on simulated
262 scRNA-seq data showed that IA-SVA outperforms existing supervised (i.e., SSVA) and
263 unsupervised (i.e., USVA) state-of-the-art methods in the estimation of hidden factors (not
264 necessarily in their elimination). Furthermore, we noted that IA-SVA is particularly effective

265 (i.e., high detection power and accuracy, and Type I error rate controlled under the nominal
266 level of 0.05) in detecting correlated factors that affect a small fraction of genes. Therefore
267 IA-SVA is an effective unsupervised alternative to existing SVA-based algorithms when the
268 goal is to accurately estimate hidden factors (and their marker genes) rather than to eliminate
269 these factors.

270 Through analyses of diverse human datasets from multiple studies, we established that
271 IA-SVA can effectively detect hidden heterogeneity in scRNA-seq data arising from a small
272 number of cells either due to technical (i.e., contamination or doublets) or biological (i.e., a
273 rare cell type) sources. In two independently generated islet scRNA-seq datasets, we showed
274 that IA-SVA detects heterogeneity stemming from compromised alpha cells (contaminated or
275 stacked), which should be excluded from the downstream analyses (Figure 2 and
276 Supplementary Figure S2). Therefore, IA-SVA provides an easy-to-apply statistical
277 framework to uncover variation in scRNA-seq data even if it is stemming from only a
278 handful of cells. This ability of IA-SVA can be effective in identifying rare cells within a
279 population of cells, where genes associated with the detected factor can uncover relevant
280 marker genes for the rare population of cells. In addition, IA-SVA can be effective in
281 detecting heterogeneity associated with cell-cycle stages without prior knowledge, therefore
282 providing an unsupervised solution to this common problem in single cell data analyses
283 (Figure 3).

284 An important feature of IA-SVA is its ability to uncover genes associated with
285 detected hidden factors. This feature can be used to detect marker genes associated with
286 different cell types. As a proof-of-concept we demonstrated this in pancreatic islet cells,
287 where we captured known marker genes (e.g., *INS, GCG*) in an unsupervised manner.
288 Moreover, genes captured by IA-SVA can be used to improve the visualization of single cells
289 into their respective clusters, as demonstrated with the analyses of islet cells from two
290 separate studies (Figure 4). Spectral tSNE[16] is a commonly used method for scRNA-seq data
291 visualization especially in the existence of confounding factors. This method regresses out
292 variation associated with known factors before data visualization. However, when a hidden
293 factor is 'wanted' (e.g., cell types) and is highly correlated with known factors, removing the
294 known factors will also diminish the ability to detect the wanted hidden factor and the genes
295 associated with this factor (e.g., marker genes for different cell types). Indeed, our analyses
296 using islet cells emphasized the importance of properly adjusting the data for known factors
297 prior to further analyses, such as data visualization (e.g., tSNE) to prevent spurious clustering

of cells due to the confounding factors (Figure 4E). IA-SVA is an alternative method that can effectively handle data with multiple confounding factors.

In summary, IA-SVA is an SVA-based unsupervised method designed to accurately estimate hidden factors (sources of variation) in single cell gene expression data while adjusting for known factors. The iterative and flexible framework of IA-SVA allows the accurate estimation of multiple and potentially correlated factors along with their statistical significance, which is the main advantage of IA-SVA over existing methods. This flexibility is more realistic given the confounded nature of known and unknown factors in single cell gene expression measurements. Therefore, IA-SVA has an improved performance over existing SVA-based methods in terms of estimating hidden sources of variation when they are correlated with each other and with known variables. IA-SVA is an effective alternative to methods developed for single cell data analyses (e.g., CellView and Seurat), especially for the analyses of complex data (i.e., data with multiple confounding and correlated factors). With the increasing amount of single cell studies and the increasing complexity of human cohorts, IA-SVA will serve as an effective statistical framework specifically designed to handle unique challenges of scRNA-seq data analyses.

Methods

IA-SVA framework.

We model the log-transformed sequencing read counts for *m* cells and *n* genes (i.e., $Y_{m\times n}$) as a combination of known and unknown variables as follows:

$$Y_{m\times n} = X_{m\times p}\beta_{p\times n} + Z_{m\times k}\delta_{k\times n} + \varepsilon_{m\times n},$$

where $X_{m\times p}$ is a matrix for p known variable(s) (e.g., group assignment for cases and controls, sex or ethnicity), $Z_{m\times k}$ is a matrix for k unknown variables and $\varepsilon_{m\times n}$ is the error term. With this model, we can account for any clinical/experimental information about samples (e.g., sex, ethnicity, age, BMI or batch) as known factors ($X_{m\times p}$) and dissect unaccounted variation in the read count data that is attributable to hidden factors ($Z_{m\times k}$).

Existing unsupervised SVA-based methods (e.g., USVA[10], RUV[13], ISVA[12]) obtain the residual matrix ($Y'_{m\times n}$) by regressing read counts ($Y_{m\times n}$) on all known factors ($X_{m\times p}$). Then, they infer the hidden factors from this residual matrix ($Y'_{m\times n}$) using dimensionality reduction algorithms (e.g., PCA, SVD or ICA). Thus, by definition, multiple hidden factors captured by

these methods are orthogonal to each other and to known variables. Therefore, if hidden factors are correlated with each other and with known factors, the direct inference from the residual matrix leads to biased estimates of hidden factors due to the orthogonality assumption.

In contrast, IA-SVA does not impose orthogonality between factors (hidden or known) and allows an unbiased estimation of correlated factors via a novel iterative framework (Figure 1). At each iteration, IA-SVA first obtains residual matrix ($Y'_{m\times n}$), i.e., read counts adjusted for all known factors ($X_{m\times p}$) including surrogate variables of unknown factors estimated from previous iterations and extracts the first principal component (PC1) from the residuals ($Y'_{m\times n}$) using SVD. Next it tests the significance of PC1 in terms of its contribution to the unmodeled variation (i.e., residual variance). Using this PC1 as a surrogate variable (as in the case of existing methods) implicitly imposes orthogonality between known and hidden factors. Instead, IA-SVA uses PC1 to infer gene weights, which are also used to infer genes associated with the hidden factor. IA-SVA relies on the fact that the first principal component (PC1) of the residual matrix is highly correlated with the hidden factor that contributes the most to the unmodeled variation in data, and thus, PC1 can be used to sort genes in terms of their relative association strength with the hidden factor. To infer these genes, IA-SVA regresses Y on PC1 and calculates the coefficient of determination (R^2) for each gene. Genes with high R^2 scores can be treated as marker genes for the factor. These R^2 scores are further utilized for an unbiased inference of the hidden factor while retaining the correlation structure between known and hidden factors. For this, IA-SVA first obtains a weighted read count matrix ($Y''_{m\times n}$) by weighing all genes with respect to their R^2 scores (i.e., $Y''_{m\times n} = Y_{m\times n}W_{n\times n}$, where W is a diagonal matrix of R^2 values). Then it conducts a SVD on $Y''_{m\times n}$ and obtains the PC1 to be used as a surrogate variable (SV) for the hidden factor. In the next iteration, IA-SVA uses this SV as an additional known factor to identify further significant hidden factors. The iterative procedure of IA-SVA is composed of six major steps as summarized in Figure 1A and below:

[Step 1] Regress $Y_{m\times n}$ on all known factors ($X_{m\times p}$), including SVs obtained from previous iterations, to obtain residuals ($Y'_{m\times n}$).

[Step 2] Conduct a SVD on the obtained residuals ($Y'_{m\times n}$) to extract the first PC (PC1).

[Step 3] Test the significance of the contribution of PC1 to the variation in residuals ($Y'_{m\times n}$) using a non-parametric permutation-based assessment [9,10,29] as explained further in the next section.

363 **[Step 4]** If PC1 is significant, regress $Y_{m\times n}$ (in this case do not use the residual matrix to be
364 able to capture factors correlated with known factors) on PC1 to compute the coefficient of
365 determination (R^2) for every gene. If PC1 is not significant, stop the iteration and conduct
366 subsequent down stream analysis using previously obtained significant SVs.
367 **[Step 5]** Weigh each gene in $Y_{m\times n}$ with respect to its R^2 value by multiplying a gene's read
368 counts ($Y_{m\times n}$) with its R^2 values ($Y''_{m\times n} = Y_{m\times n}W_{n\times n}$). The highly weighted genes in this
369 framework serve as the genes affected by the hidden factor.
370 **[Step 6]** Conduct a second SVD on this weighted read counts matrix ($Y''_{m\times n} = Y_{m\times n}W_{n\times n}$) to
371 obtain PC1, which will be used as the surrogate variable (SV) for the hidden factor.

372 At the end of this six-step procedure, IA-SVA uses the detected SV (if significant) as
373 an additional known factor in the next iteration. The algorithm stops, when no more
374 significant PC1s are detected in Step 3. Significant SVs obtained via IA-SVA can be used in
375 subsequent analyses. If an SV arises from an unwanted factor (e.g., cell contamination), these
376 SVs can be included as covariates in the model to remove the unwanted variation or to filter
377 out contaminated cells. In single cell data significant SVs could also explain 'wanted'
378 biological factors (e.g., different cell types) and genes associated with such SVs can be
379 further evaluated to discover novel biology from these complex datasets.

380 **Assessing the significance of hidden factors.**

381 To test the significance of the contribution of a hidden factor estimate (i.e., PC1 obtained in
382 Step 2) to the residual variation, we used the permutation based significance test as
383 previously applied in the surrogate variable analysis [10,29]. Unlike SVA [10], which tests all
384 putative hidden factors at once, IA-SVA assesses the significance of hidden factors one at a
385 time during the corresponding iteration (always for the PC1 detected in that iteration). Briefly,
386 IA-SVA i) conducts a SVD on the residual matrix obtained from Step 1, ii) computes the
387 proportion of variation in this matrix explained by the first singular vector (i.e., PC1) and iii)
388 compares this proportion against the values obtained from permuted residual matrices, as
389 further explained below:

390 **[Step 1]** Conduct a SVD on the residual matrix ($Y'_{m\times n}$).
391 **[Step 2]** Calculate the proportion of residual variance explained by the first singular vector
392 (PC1) using the test statistic: $T_{obs} = \frac{\lambda_1^2}{\sum_k \lambda_k^2}$, where λ_k is the k-th singular value.

393 **[Step 3]** Generate a permuted residual matrix by i) permuting each row of the log-
394 transformed read count matrix $Y_{m\times n}$ and regressing the permuted read count matrix on all
395 known factors ($X_{m\times p}$) to obtain fitted residuals.
396 **[Step 4]** Repeat Step 3 *M* times and generate an empirical null distribution of the test statistic
397 by calculating ($T_i^0, i = 1, \ldots, M$) for the *M* permuted residual matrices.
398 **[Step 5]** Compute the empirical p-value for the first singular vector (PC1) by counting the
399 number of times the null statistics (T_i^0) exceeds the observed one (T_{obs}) divided by the
400 number of permutations (*M*).

401 **scRNA-seq data simulation.**

402 To eliminate the potential bias in data simulations and make simulation studies more
403 objective [30], we used a third-party simulation software (Polyester R package [31]) and study
404 design (http://jtleek.com/svaseq/simulateData.html) and simulated scRNA-seq data to test IA-
405 SVA's performance. The original simulation design is slightly modified to reflect
406 characteristics of scRNA-seq data for high dropout rate (i.e., excessive number of zeros in the
407 data) and multiple hidden factors highly correlated with known factors. First, to simulate high
408 dropout rates (proportion of zero counts = ~70%), we estimated Polyster's zero-inflated
409 negative binomial model parameters (i.e., p_0: probabilities that the count will be zero, mu:
410 mean of the negative binomial, size: size of the negative binomial) from real-world scRNA-
411 seq data from human pancreatic islets using the Fludigm's C1 platform [17]. Using these
412 estimated model parameters, we simulated expression data for *m* cells and *n* genes under two
413 hypotheses: 1) the null hypothesis: no hidden sources of variation, and 2) the alternative
414 hypothesis: three hidden factors with two values (-1 vs. 1). Under both scenarios, we
415 simulated a primary variable of interest (i.e., case vs. control) and simulated 10% of genes to
416 be differentially expressed between the two groups. Under the alternative hypothesis, we
417 simulated three hidden factors that affect 30%, 20% and 10% of randomly chosen genes
418 respectively and simulated two different scenarios where these factors are moderately
419 correlated ($|r|$=~0.3-0.6) or weakly correlated ($|r|$<0.3) with the group variable.

420 **Data processing and normalization.**

421 In all analyses, we filtered out low-expressed genes with read counts <= 5 in less than three
422 cells and normalized the retained gene expression counts using SCnorm[19] with default
423 settings for further analyses. For single cell data visualization examples, we normalized gene

read counts by dividing each cell column by its total counts then multiplying median of library size, which is similar to the default normalization method "LogNormalize" implemented in Seurat [16].

Availability of data and methods.

An R package for IA-SVA with example case scenarios is freely available from https://github.com/UcarLab/IA-SVA. The published data sets analyzed in this study including single-cell RNA sequencing read counts and annotations describing samples and experiment settings are included in an R data package (iasvaExamples) deposited at https://github.com/dleelab/iasvaExamples.

References

1 Tung, P.-Y. *et al.* Batch effects and the effective design of single-cell gene expression studies. *bioRxiv*, 062919 (2016).

2 Kowalczyk, M. S. *et al.* Single-cell RNA-seq reveals changes in cell cycle and differentiation programs upon aging of hematopoietic stem cells. *Genome research* **25**, 1860-1872 (2015).

3 Stegle, O., Teichmann, S. A. & Marioni, J. C. Computational and analytical challenges in single-cell transcriptomics. *Nat Rev Genet* **16**, 133-145, doi:10.1038/nrg3833 (2015).

4 Villani, A. C. *et al.* Single-cell RNA-seq reveals new types of human blood dendritic cells, monocytes, and progenitors. *Science* **356**, doi:10.1126/science.aah4573 (2017).

5 Ilicic, T. *et al.* Classification of low quality cells from single-cell RNA-seq data. *Genome Biol* **17**, 29, doi:10.1186/s13059-016-0888-1 (2016).

6 Buettner, F. *et al.* Computational analysis of cell-to-cell heterogeneity in single-cell RNA-sequencing data reveals hidden subpopulations of cells. *Nat Biotechnol* **33**, 155-160, doi:10.1038/nbt.3102 (2015).

7 McDavid, A., Finak, G. & Gottardo, R. The contribution of cell cycle to heterogeneity in single-cell RNA-seq data. *Nat Biotechnol* **34**, 591-593, doi:10.1038/nbt.3498 (2016).

8 Hicks, S. C., Teng, M. & Irizarry, R. A. On the widespread and critical impact of systematic bias and batch effects in single-cell RNA-Seq data. *bioRxiv*, doi:10.1101/025528 (2015).

9 Leek, J. T. & Storey, J. D. Capturing heterogeneity in gene expression studies by surrogate variable analysis. *PLoS Genet* **3**, 1724-1735, doi:10.1371/journal.pgen.0030161 (2007).

10 Leek, J. T. & Storey, J. D. A general framework for multiple testing dependence. *Proc Natl Acad Sci U S A* **105**, 18718-18723, doi:10.1073/pnas.0808709105 (2008).

11 Leek, J. T. svaseq: removing batch effects and other unwanted noise from sequencing data. *Nucleic Acids Res* **42**, doi:10.1093/nar/gku864 (2014).

12 Teschendorff, A. E., Zhuang, J. & Widschwendter, M. Independent surrogate variable analysis to deconvolve confounding factors in large-scale microarray profiling studies. *Bioinformatics* **27**, 1496-1505, doi:10.1093/bioinformatics/btr171 (2011).

13 Risso, D., Ngai, J., Speed, T. P. & Dudoit, S. Normalization of RNA-seq data using factor analysis of control genes or samples. *Nat Biotechnol* **32**, 896-902, doi:10.1038/nbt.2931 (2014).

14 Gagnon-Bartsch, J. A. & Speed, T. P. Using control genes to correct for unwanted variation in microarray data. *Biostatistics* **13**, 539-552, doi:10.1093/biostatistics/kxr034 (2012).

15 Maaten, L. V. D. Accelerating t-SNE using tree-based algorithms. *J. Mach. Learn. Res.* **15**, 3221-3245 (2014).

16 Macosko, E. Z. *et al.* Highly Parallel Genome-wide Expression Profiling of Individual Cells Using Nanoliter Droplets. *Cell* **161**, 1202-1214, doi:10.1016/j.cell.2015.05.002 (2015).
17 Lawlor, N. *et al.* Single cell transcriptomes identify human islet cell signatures and reveal cell-type-specific expression changes in type 2 diabetes. *Genome Res*, doi:10.1101/gr.212720.116 (2016).
18 Xin, Y. *et al.* RNA Sequencing of Single Human Islet Cells Reveals Type 2 Diabetes Genes. *Cell Metab* **24**, 608-615, doi:10.1016/j.cmet.2016.08.018 (2016).
19 Bacher, R. *et al.* SCnorm: robust normalization of single-cell RNA-seq data. *Nat Methods* **14**, 584-586, doi:10.1038/nmeth.4263 (2017).
20 Xin, Y. *et al.* Use of the Fluidigm C1 platform for RNA sequencing of single mouse pancreatic islet cells. *Proc Natl Acad Sci U S A* **113**, 3293-3298, doi:10.1073/pnas.1602306113 (2016).
21 Wang, Y. J. *et al.* Single-Cell Transcriptomics of the Human Endocrine Pancreas. *Diabetes* **65**, 3028-3038, doi:10.2337/db16-0405 (2016).
22 Patel, A. P. *et al.* Single-cell RNA-seq highlights intratumoral heterogeneity in primary glioblastoma. *Science* **344**, 1396-1401, doi:10.1126/science.1254257 (2014).
23 Kanehisa, M., Sato, Y., Kawashima, M., Furumichi, M. & Tanabe, M. KEGG as a reference resource for gene and protein annotation. *Nucleic Acids Res* **44**, D457-462, doi:10.1093/nar/gkv1070 (2016).
24 Gene Ontology, C. Gene Ontology Consortium: going forward. *Nucleic Acids Res* **43**, D1049-1056, doi:10.1093/nar/gku1179 (2015).
25 Lun, A. T., McCarthy, D. J. & Marioni, J. C. A step-by-step workflow for low-level analysis of single-cell RNA-seq data with Bioconductor. *F1000Res* **5**, 2122, doi:10.12688/f1000research.9501.2 (2016).
26 Bolisetty, M. T., Stitzel, M. L. & Robson, P. CellView: Interactive Exploration Of High Dimensional Single Cell RNA-Seq Data. *bioRxiv*, doi:10.1101/123810 (2017).
27 Lawlor, N., Khetan, S., Ucar, D. & Stitzel, M. L. Genomics of Islet (Dys)function and Type 2 Diabetes. *Trends Genet* **33**, 244-255, doi:10.1016/j.tig.2017.01.010 (2017).
28 Proserpio, V. & Lonnberg, T. Single-cell technologies are revolutionizing the approach to rare cells. *Immunol Cell Biol* **94**, 225-229, doi:10.1038/icb.2015.106 (2016).
29 Buja, A. & Eyuboglu, N. Remarks on Parallel Analysis. *Multivariate Behav Res* **27**, 509-540, doi:10.1207/s15327906mbr2704_2 (1992).
30 Gelman, A. & Hennig, C. Beyond subjective and objective in statistics. *Journal of the Royal Statistical Society: Series A (Statistics in Society)*, n/a-n/a, doi:10.1111/rssa.12276 (2017).
31 Frazee, A. C., Jaffe, A. E., Langmead, B. & Leek, J. T. Polyester: simulating RNA-seq datasets with differential transcript expression. *Bioinformatics* **31**, 2778-2784, doi:10.1093/bioinformatics/btv272 (2015).

Acknowledgements

We thank the Jackson Laboratory Computational Science group, Ucar and Stitzel lab members for constructive feedback throughout this project. We thank Jane Cha, JAX scientific illustrator, for her help with Figure 1. This study was made possible by generous financial support of the National Institute of General Medical Sciences (NIGMS) under award number GM124922 (to DU) and by the Jackson Laboratory Scientific Services Innovation Fund (to D.L. and D.U.) Opinions, interpretations, conclusions, and

recommendations are solely the responsibility of the authors and do not necessarily represent the official views of the National Institutes of Health (NIH).

Author Contributions

D.L. and D.U. designed the project, generated the figures and wrote the manuscript. D.L. developed the statistical framework and run the data analyses. M.B. provided advice on data analyses and interpretation of results. A.C. contributed to the data pre-processing and the generation of the R package. All authors read and approved this manuscript prior to submission.

Additional Information

Supplementary information accompanies this paper at http://www.nature.com/srep.

Competing financial interests: The authors declare no competing financial interests.

539 ## Figure Legends

540 **Figure 1. IA-SVA is a robust statistical framework to detect and estimate multiple and**
541 **correlated hidden sources of variation. (A)** Six-step IA-SVA procedure. IA-SVA computes
542 the first principal component (PC1) from read counts adjusted for all known factors and tests
543 its significance [Steps 1-3]. If significant, IA-SVA uses this PC1 to infer a set of genes
544 associated with the hidden factor [Steps 4-5] and obtain a surrogate variable (SV) to represent
545 the hidden factor using these genes [Step 6]. **(B)** IA-SVA uses single-cell gene expression
546 data matrix and known factors to detect hidden sources of variation (e.g., cell contamination,
547 cell-cycle status, and cell type). If these factors match to a biological variable of interest (e.g.,
548 cell type assignment), genes highly correlated with the factor can be detected and used in
549 downstream analyses (e.g., data visualization).

550 **Figure 2. IA-SVA can detect heterogeneity originating from potentially contaminated**
551 **alpha cells. (A)** Outlier alpha cells captured using IA-SVA and same cells marked in
552 respective (**C**) PCA, (**D**) USVA, and (**E**) tSNE analyses. Cells are clustered into two groups
553 (red vs. gray dots) based on IA-SVA's surrogate variable 2 (SV2 > 0.1). In PCA, PC1 was
554 discarded since it explains the geometric library size. (**B**) Hierarchical clustering of alpha
555 cells using 27 genes significantly associated with SV2 (FDR < 0.05 and R^2 > 0.6) (ward.D2
556 and cutree_cols =2). 6 cells clearly separated from the rest of the alpha cells based on the
557 expression of these 27 genes.

558 **Figure 3. IA-SVA can detect heterogeneity stemming from differences in cell-cycle stage.**
559 (**A**) Visualization of glioblastoma cells based on IA-SVA-detected factors (SV1 and SV2).
560 Same cells are marked in respective analyses with (**C**) PCA, (**D**) USVA, and (**E**) tSNE
561 analyses. IA-SVA's SV1 clearly separates cells into two groups (red vs. blue dots, SV1 > 0.1).
562 Other methods failed to clearly detect this cell-cycle related heterogeneity. **(B)** Hierarchical
563 clustering on 119 genes significantly associated (FDR < 0.05 and R^2 > 0.3) with IA-SVA's
564 SV2 confirms the separation of cells based on these genes (ward.D2 and cutree_cols = 2). (**F**)
565 IA-SVA's SV1 can segregate cells based on their cell-cycle-stage as predicted by SCRAN.

566 **Figure 4. IA-SVA based gene selection enhances single cell data visualization. (A)** tSNE
567 analyses using all expressed genes in human islet data (tSNE). Cells are color-coded based on
568 the original cell-type assignments. Note that cells are not effectively clustered with respect to
569 their assigned cell types. (**B**) Hierarchical clustering using genes (n=92) selected by IA-SVA
570 clearly separate cell types (ward.D2 and cutree_cols=3). Known marker genes (e.g., *INS*) are

highlighted in red color. (**C)** tSNE analyses using the 92 IA-SVA genes (IA-SVA+tSNE). Note the improved grouping of cell types into discrete clusters. (**D)** tSNE analyses using top variable genes in a second and bigger islet scRNA-seq data. Note that cells are not effectively clustered with respect to their assigned cell types just using tSNE. (**E)** tSNE analyses repeated using genes (n=57) obtained via IA-SVA (IA-SVA+tSNE). Note the improved clustering of different cell types into discrete clusters. (**F**) tSNE analyses using 1000 most over-dispersed genes (CellView**)**. (**G**) tSNE analyses on significant PCs obtained from highly over-dispersed genes (Spectral tSNE).

Tables

	USVA	SSVA	IA-SVA	USVA	SSVA	IA-SVA
	$\|r\| = 0.3 \sim 0.6$			$\|r\| < 0.3$		
Power*(F1**)	1	1	1	1	1	1
Power (F2)	1	1	1	1	1	1
Power (F3)	0.78	0.78	0.87	1	1	1
Cor***(F1)	0.93	0.95	0.95	0.98	0.98	1
Cor (F2)	0.72	0.75	0.94	0.94	0.94	0.99
Cor (F3)	0.75	0.78	0.95	0.93	0.93	0.98

	USVA	SSVA	IA-SVA
Type I error*	0.09	0.09	0.04

*Nominal Type I error rate: 0.05

**F1, F2, F3 refers to Factor1, Factor2, and Factor3

***Average of the absolute Pearson correlation coefficients between the true factor and the estimated factor is used as the accuracy measure.

Table 1. IA-SVA accurately captures unknown sources of variation while controlling Type I error rate at a nominal level. Empirical power, Type I error rate, and the accuracy of estimates for IA-SVA, SSVA, and USVA assessed using simulated single-cell gene expression data. Alternative scenarios are simulated in which hidden factors are moderately ($|r|$=~0.3-0.6, first three columns) or weakly ($|r|$<0.3, last three columns) correlated with the group variable. IA-SVA outperforms alternative methods especially while detecting variation stemming from a smaller fraction of genes (10%) and especially when factors are correlated.

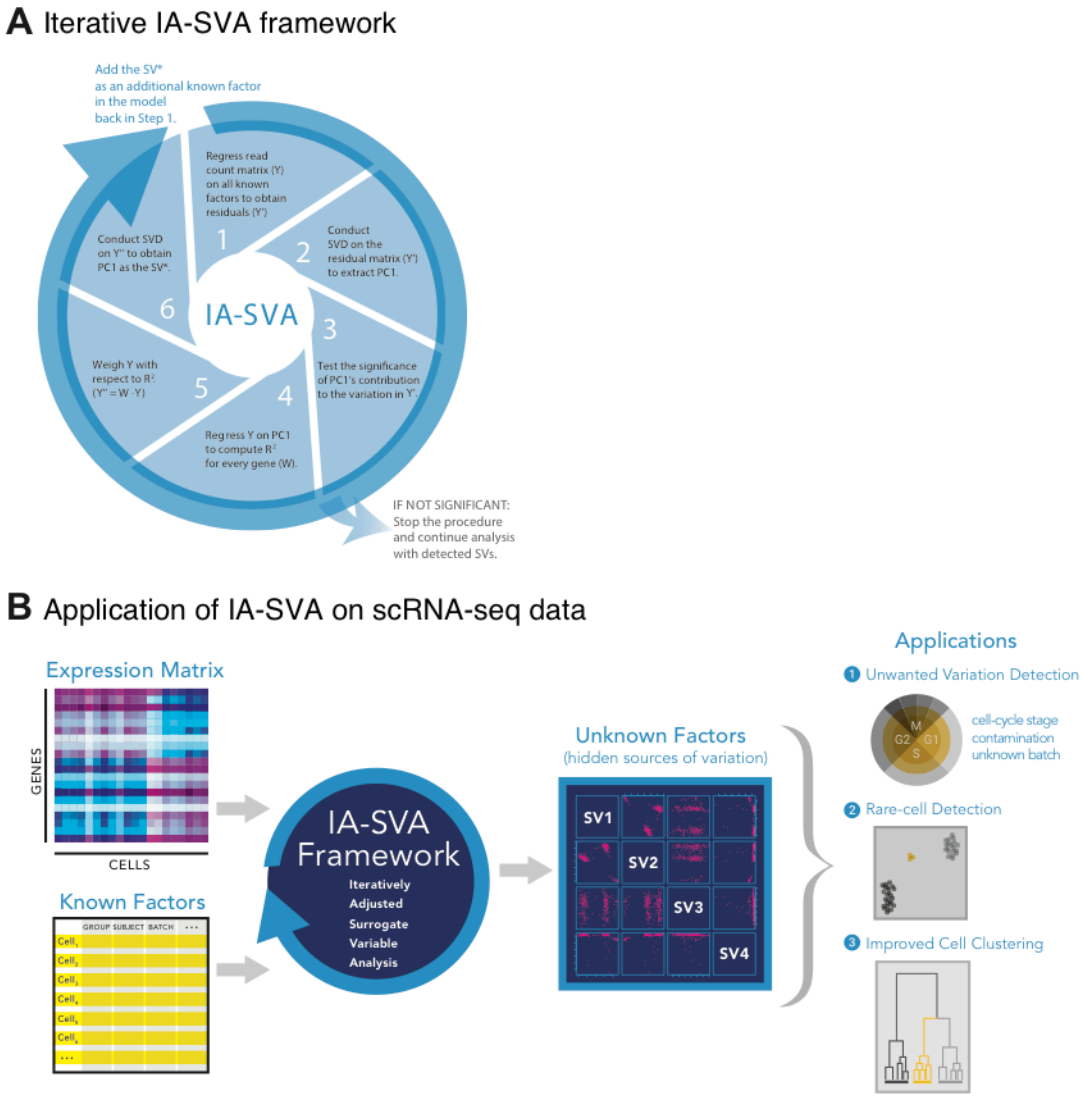

Figure 1. IA-SVA is a robust statistical framework to detect and estimate multiple and correlated hidden sources of variation. (A) Six-step IA-SVA procedure. IA-SVA computes the first principal component (PC1) from read counts adjusted for all known factors and tests its significance [Steps 1-3]. If significant, IA-SVA uses this PC1 to infer a set of genes associated with the hidden factor [Steps 4-5] and obtain a surrogate variable (SV) to represent the hidden factor using these genes [Step 6]. **(B)** IA-SVA uses single-cell gene expression data matrix and known factors to detect hidden sources of variation (e.g., cell contamination, cell-cycle status, and cell type). If these factors match to a biological variable of interest (e.g., cell type assignment), genes highly correlated with the factor can be detected and used in downstream analyses (e.g., data visualization).

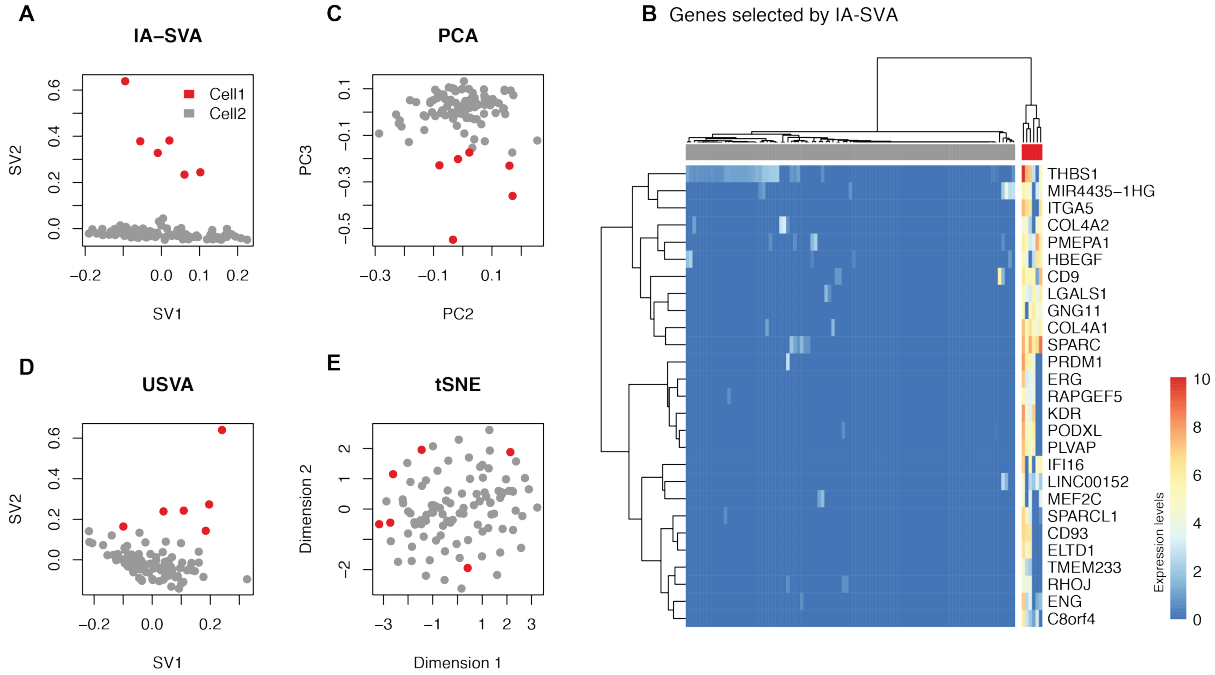

Figure 2. IA-SVA can detect heterogeneity originating from potentially contaminated alpha cells. (A) Outlier alpha cells captured using IA-SVA and same cells marked in respective (**C**) PCA, (**D**) USVA, and (**E**) tSNE analyses. Cells are clustered into two groups (red vs. gray dots) based on IA-SVA's surrogate variable 2 (SV2 > 0.1). In PCA, PC1 was discarded since it explains the geometric library size. (**B**) Hierarchical clustering of alpha cells using 27 genes significantly associated with SV2 (FDR < 0.05 and R^2 > 0.6) (ward.D2 and cutree_cols =2). 6 cells clearly separated from the rest of the alpha cells based on the expression of these 27 genes.

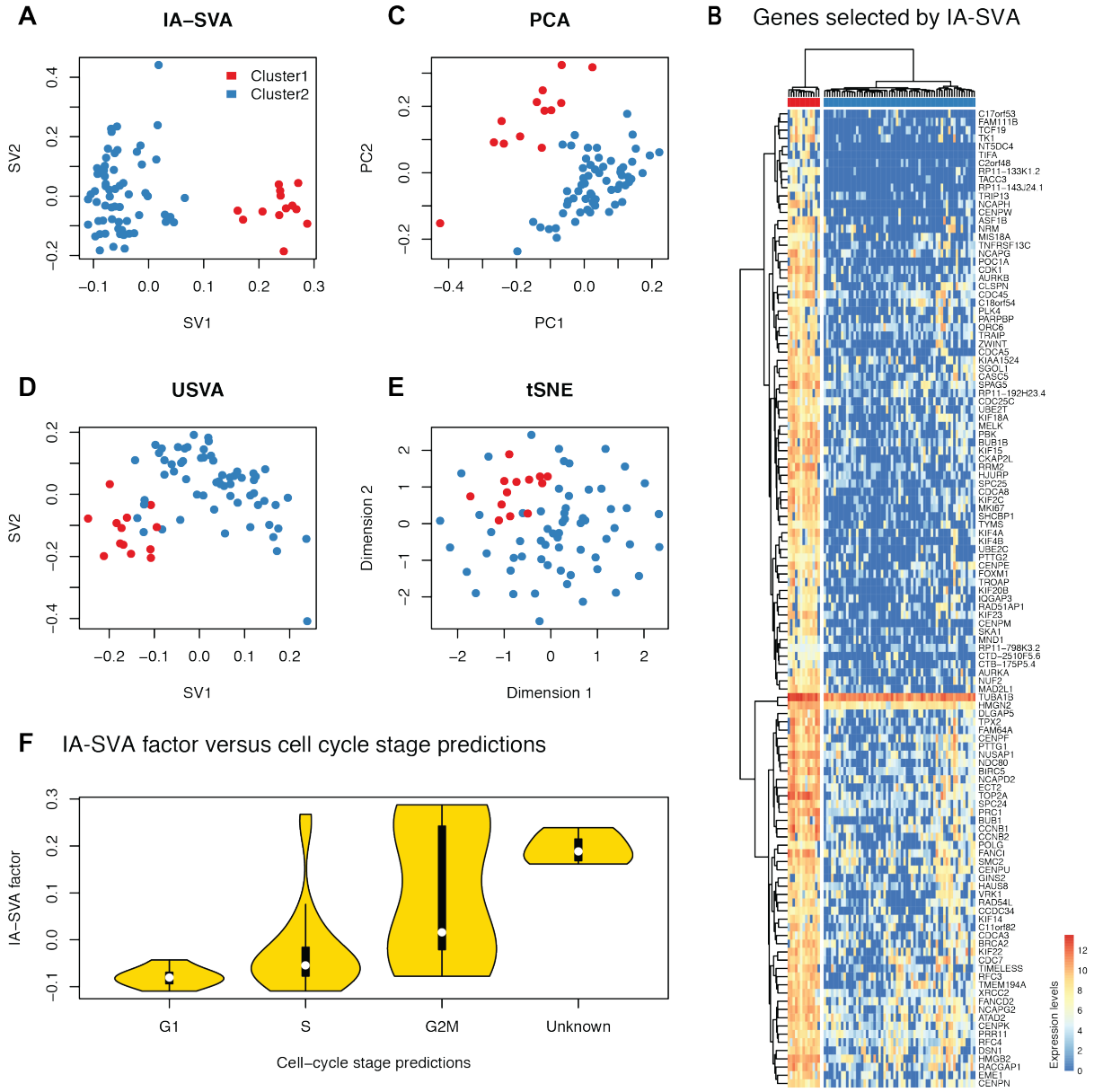

Figure 3. IA-SVA can detect heterogeneity stemming from differences in cell-cycle stage. (**A**) Visualization of glioblastoma cells based on IA-SVA-detected factors (SV1 and SV2). Same cells are marked in respective analyses with (**C**) PCA, (**D**) USVA, and (**E**) tSNE analyses. IA-SVA's SV1 clearly separates cells into two groups (red vs. blue dots, SV1 > 0.1). Other methods failed to clearly detect this cell-cycle related heterogeneity. (**B**) Hierarchical clustering on 119 genes significantly associated (FDR < 0.05 and R^2 > 0.3) with IA-SVA's SV2 confirms the separation of cells based on these genes (ward.D2 and cutree_cols = 2). (**F**) IA-SVA's SV1 can segregate cells based on their cell-cycle-stage as predicted by SCRAN.

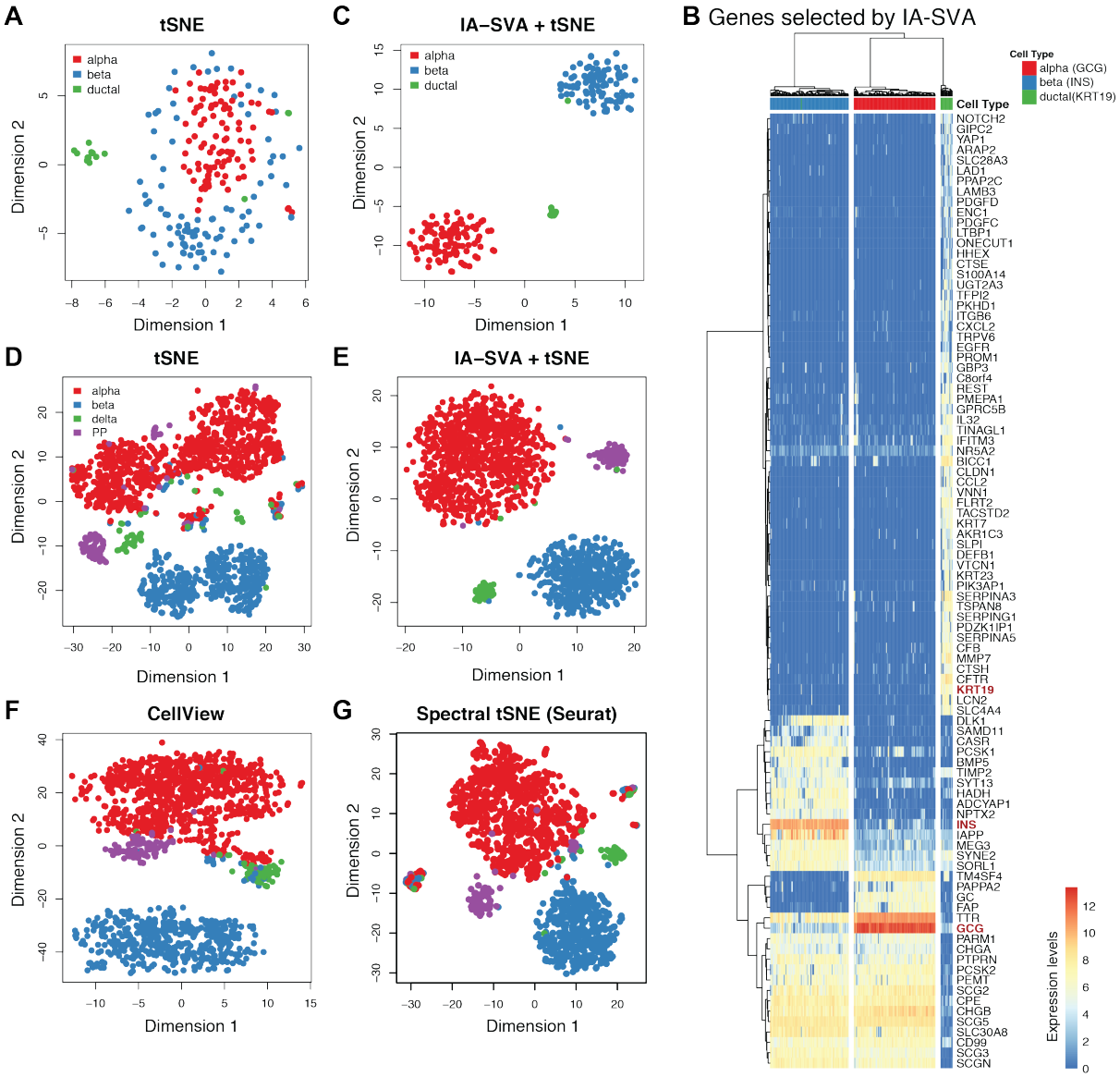

Figure 4. IA-SVA based gene selection enhances single cell data visualization. (A) tSNE analyses using all expressed genes in human islet data (tSNE). Cells are color-coded based on the original cell-type assignments. Note that cells are not effectively clustered with respect to their assigned cell types. **(B)** Hierarchical clustering using genes (n=92) selected by IA-SVA clearly separate cell types (ward.D2 and cutree_cols=3). Known marker genes (e.g., *INS*) are highlighted in red color. **(C)** tSNE analyses using the 92 IA-SVA genes (IA-SVA+tSNE). Note the improved grouping of cell types into discrete clusters. **(D)** tSNE analyses using top variable genes in a second and bigger islet scRNA-seq data. Note that cells are not effectively clustered with respect to their assigned cell types just using tSNE. **(E)** tSNE analyses repeated using genes (n=57) obtained via IA-SVA (IA-SVA+tSNE). Note the improved clustering of different cell types into discrete clusters. **(F)** tSNE analyses using 1000 most over-dispersed genes (CellView). **(G)** tSNE analyses on significant PCs obtained from highly over-dispersed genes (Spectral tSNE).